Vol. 14(2), pp. 12-23, July-December, 2024
DOI: 10.5897/JCEMS2023.0375
Article Number: 52065A572323
ISSN: 2141-6605

http://www.academicjournals.org/JCEMS

ACADEMIC JOURNALS
expand your knowledge

Journal of Chemical Engineering and Materials Science

Full Length Research Paper

Preparation and manufacturing of nanomembranes based on ramie fiber using electrospinning technique

Sudirman Habibie*, Riesma Tasomara, Seto Roseno, Mohammad Hamzah, Lukmana, Trisna Mardiana and Arif Rachman Hakim

Research Centre for Advanced Material, National Research and Innovation Agency, Building 224, PUSPIPTEK, South Tangerang 15314, Indonesia.

Received 8 October, 2023; Accepted 7 March, 2024

In this study, ramie fibers were used to fabricate nanomembranes, which are expected to be able to filter micron/nano-sized particles. The ramie fibers were processed into cellulose pulp and processed into cellulose acetate. Ramie cellulose acetate is the basic material for making nanomembranes through an electrospinning process. Nanomembrane characterization was carried out using FTIR, thermogravimetry analysis (TGA), scanning electron microscopy (SEM), Keyence microscopy and tensile strength. Observation of the diameter of the fibers on the nanomembrane using a polarizing microscope indicated that the higher the electrospinning voltage, the higher the fiber production; however, there was a decrease in the number of fibers with smaller diameters. Meanwhile, cellulose acetate (CA) nanomembranes with the addition of Zn (5%) produced nanomembranes with better performance, where the tensile strength is 2 times and the elongation was 3.5 times compared to the CA nanomembrane itself. In addition, it also has indications of water- and fire-resistant properties as well as possible antimicrobial properties (needs further testing) on the nanomembrane. Thus, CA - Zn based nanomembrane may have potential as a filter in medical masks and firefighting masks.

Key words: Ramie fiber, cellulose acetate, zinc acetate, nanomembrane, electrospinning.

INTRODUCTION

The research and development of membrane technology for nanotechnology continues to grow in line with the demands of today's technological needs to produce environmentally friendly products. Membranes are widely used in the fields of health, food, water and wastewater treatment, and the chemical industry, as well as in other fields of biotechnology.

Natural fibers have recently become popular as an alternative to replace synthetic fibers as industrial raw materials, considering that they have inherent properties such as biodegradability, renewability, and abundant availability compared to synthetic fibers (Habibie et al., 2021a). Natural polymer raw materials, which are typically used for manufacturing cellulose acetate as a membrane material, are natural cotton fibers. Based on the results of previous studies, cellulose acetate can be produced through acetylation via wood pulp dissolution.

In recent years, ramie, a natural fiber, has received

*Corresponding author. E-mail: sudirmanhabibie@yahoo.com.

significant attention from stakeholders in Indonesia as an industrial raw material, particularly in the textile industry (Habibie et al., 2021b). This paper describes the potential of ramie fiber, which can be used as a raw material for the manufacture of dissolved pulp, as an ingredient in the manufacture of cellulose acetate, and its prospects for cellulose acetate membranes. The resulting membrane potentials were evaluated and compared with those of commercial membranes.

Renewable technology is rapidly growing and is currently the focus of the world. One of the renewable technologies being developed is the separation technology using membranes that utilize renewable materials, such as natural polymers (Lankaster, 2002). Separation technology using electrospinning is a green route for preparing cellulose acetate particles from ramie fibers (Liu et al., 2007).

Membrane separation technology has been widely developed as an alternative to the conventional separation processes. This technology has advantages over conventional techniques, such as the low energy required, ability to run continuously, ability to be combined with other separation processes, lack of additives, suitability for compounds that are not heat-resistant, and lack of waste production (Nunes, 2001). With these advantages, membrane technology has been widely applied in various fields, including industrial, chemical and pharmaceutical fields; in the field of waste treatment; and environmental technology in the field of oil processing, namely vegetable oil processing (Coutinho Cesar de, 2009). However, in Indonesia, the development of membrane technology is not as rapid as in other countries because membrane materials must still be imported.

Membrane materials can be made of ceramics, silica, zeolites, metals, glass or polymers (Drioli and Lidietta, 2010). Biopolymers such as chitosan (Astuti, 2008), jelly (Setyaningrum et al., 2017), and cellulose (Yuan et al., 2009) have been widely developed as membrane base materials. In particular, cellulose has great potential as an alternative to membrane materials or their derivatives such as cellulose acetate. Indonesia has a wealth of potential natural resources as a cellulose material, including ramie fiber, which contains up to 72 to 97% cellulose.

Cellulose acetate is advantageous as a basic material for making membranes because it has an asymmetric structure with a very thin active layer, can hold dissolved materials on a rough buffer layer, is resistant to precipitation, and produces a balance between hydrophilic and hydrophobic properties (Kumano and Fujiwara, 2008). An ideal membrane requires adaptable surface properties, that is, hydrophobic or hydrophilic, a large specific surface area, high porosity with the desired pore size, and a high density of reactive groups, in addition to the general requirements for good chemical and mechanical resistance (Xia et al., 2003; Suen et al., 2003; Karakoc et al., 2004). We developed a simple and inexpensive method for fabricating hydrophobic/ hydrophilic surfaces on CA membranes. The hydrophobic/ hydrophilic surface exhibits long-term stability in pure water, and it is envisaged that this technique will enable the large-scale production of hydrophobic/hydrophilic materials for industrial engineering.

Electrospinning is a technology that is generally used for the formation of electrostatic fibers that utilizes electricity to produce polymer fibers with nanosized diameters using polymer compounds, natural polymers and synthetic polymers. The electrospinning process has received considerable attention owing to the flexibility of the materials with which it can be used and its ability to produce fibers in the submicron range. Submicron fibres are fibres that would be difficult to achieve using conventional mechanical fibre spinning methods. This technique has been used for more than 60 years in the textile industry to manufacture non-woven fiber fabrics. In recent years, there has been increasing interest in utilizing this technology to produce nanofibers. Increasing interest in the manufacture of nanofibers has led to the use of various types of natural and synthetic polymers for tissue technology. The natural and synthetic polymers used include polyurethane (Stankus et al., 2004), collagen (Matthews et al., 2002), hyaluronic acid (Um et al., 2004), cellulose (Ma et al., 2005), chitosan/collagen (Chen et al., 2002), and cassava starch (Sunthornvarabhas et al., 2011). To date, electrospinning has been the only technique available for the production of very small-diameter fibers (Dersch et al., 2005), and electrospinning can be an alternative to improve the performance of nanofiber membranes. Electrospun nanofibers have a large surface-area-to-volume ratio, adaptable porous structure, and a simple preparation process, making them excellent candidates for filtration materials. Therefore, electrospun nanofibers have attracted significant public attention for air-filtration applications (Lu et al., 2021).

Making nanomembranes using electrospinning

A membrane is defined as a thin layer or film whose interior is porous so that it can pass through certain components but is a barrier to other materials or components. A more general definition of a membrane is a selective barrier between two phases. Membranes can be divided into several groups based on the presence of the membrane, the method of manufacture, the morphology of the membrane, the density of the membrane and the function of the membrane. Membranes can be classified into several groups based on their functions, namely, microfiltration, ultrafiltration, reverse osmosis, electrodialysis, and pervaporation membranes.

Electrospinning is a method in which materials in a

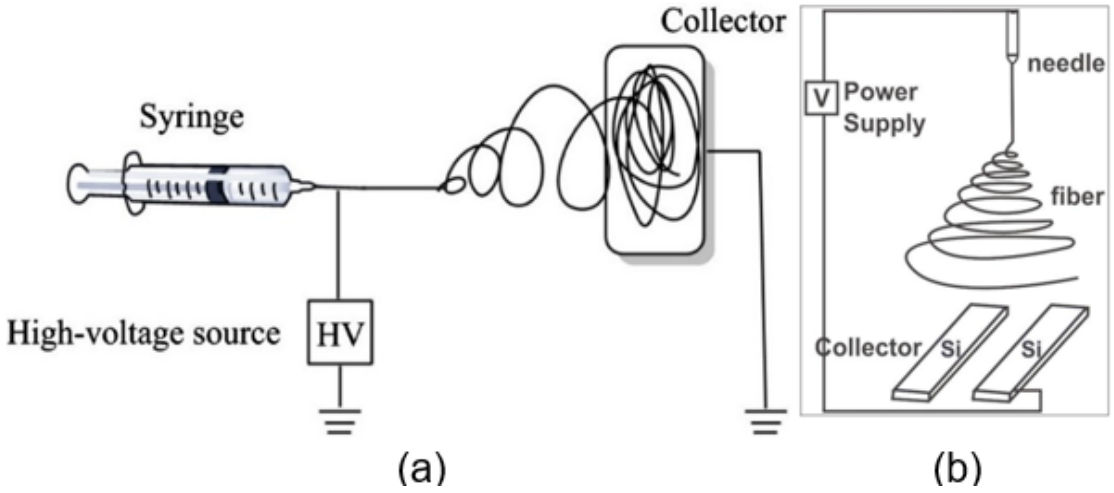

Figure 1. Schematic drawing of the electrospinning process: (a) typical electrospinning apparatus and its components and (b) modification of the collector for aligning electrospun nanofibers.

solution or melt are formed into nano- or microsized continuous fibers. Figure 1 shows the schematic of the electrospinning setup. It consists of three main components: A high-voltage source, syringe pump and collector.

Electrospinning is based on the application of a strong electric field. The solution or polymer melt was placed in a syringe pump. When a high voltage is applied, usually between 1 and 30 kV, the droplets from the polymer solution pendant become highly electrified and the induced charge is evenly distributed over the surface. The liquid drop is deformed into a cone-shaped object known as a Taylor cone by an electrostatic field (Taylor, 1969). When the voltage exceeds the threshold value, the electric force overcomes the surface tension of the droplet, and one or more charged solution jets are ejected from the tip of the droplet depending on the intensity of the electric field.

As the jet moves towards the collecting metal screen (opposite electrode), the solvent evaporates, and a non-woven cloth mat forms on the screen (Zeng et al., 2003).

The electrospinning technique involves the introduction of a strong potential difference between the polymer solution flowing through the capillary tip and metal collector (Deitzel et al.,2001). A typical electrospinning setup requires a high-voltage power supply, syringe, flat-tip needle, and collector conductor (Figure 1a) (Zhang et al., 2009). However, the basic equipment can be modified for various applications such as using multiple syringes (to make blended fibers) or rotating roller collectors (to make nanofiber-coiled materials). Conventionally, electrospun materials contain an array of nonwoven nanofibers. Electrospinning with two electrode strips (Figure 1b) can be used to collect parallel fibers (Li et al., 2003).

One of the widely known membrane manufacturing technologies is the chemical method, but this method is quite difficult to produce nano-sized membranes and is not environmentally friendly. This gave us the idea to utilize the electrospinning method, by using ramie fiber as a source of cellulose raw material to produce nanomembranes. It is hoped that the resulting nanomembrane can be used in the medical field or others.

In this research, nanofiber membranes were fabricated using electrospinning techniques so that they are expected to provide optimal performance for use as filters in the industrial sector, especially in the medical sector. This is in accordance with what was researched by Zakrzewska et al. (2022), that the flexibility of electrospun polymer nanofibers determines their suitability as a material for making “smart” filter media.

MATERIALS

Ramie fiber material was obtained from UKM Rabersa Wonosobo. The chemicals used are as follows; solid NaOH, Zn Acetate for analysis, 100% glacial acetic acid, 37% sulfuric acid, 40% hydrochloric acid, 99.6% acetic anhydride, and all these chemicals are from the Merck brand. These chemicals were not subjected to further characterization. The equipment used is laboratory equipment such as supporting glasses, measuring cups, pipettes, stirrers, heaters, filter paper, main equipment for electrospinning machines, and test equipment such as FTIR, TGA, SEM, Droplet test and tensile test.

METHODS

First, preparation for the extraction of cellulose from ramie fiber is shown in Figure 2. Several grams of ramie fiber are hydrolyzed with acid (HCl) (Handayani et al., 2018) to convert ramie fiber into a form of cellulose with a lower molecular weight and simultaneously remove non-cellulose substances. Furthermore, hydrolysis of cellulose is carried out by delignilization using NaOH (Muryanto et

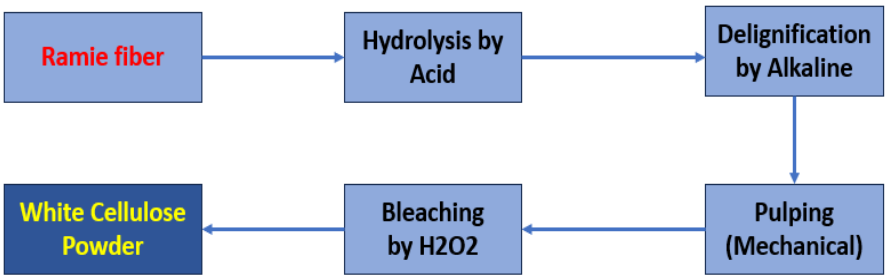

Figure 2. Extraction of cellulose from ramie fiber.

al., 2016) to remove lignin and other purities, although some lignin may have been removed at the hydrolysis stage. Subsequently, the delignized cellulose was mechanically pulped and bleached using a H_2O_2 solution to obtain white cellulose powder. This cellulose powder was used to manufacture the cellulose acetate.

One gram of ramie cellulose was added to 40 mL distilled water and stirred for 30 min. Subsequently, the strain was dried. Dried cellulose was added to 20 ml of glacial acetic acid and stirred for 30 min. Then, 0.1 ml was added to the mixture of cellulose and glacial acetic acid and the temperature to 80°C. Next, 6 ml of acetic anhydride was added to the mixture and stirred for 30 min. Distilled water: acetone 1:5 (8 ml:40 ml) was added to the final mixture, and the mixture was stirred for 30 min.

The precipitate was then filtered and washed until the pH reached approximately 6 to 7. Finally, the precipitate was dried at 105°C for 3 h. The precipitate was used to determine the functional groups. Distilled water and acetic acid were selected as the developer because of their short development time, high degree of acetylation, and relative environmental friendliness (Liu et al., 2007).

To optimize the reaction for the formation of cellulose acetate, research was carried out at several reaction temperatures, namely 40 and 80°C, then characterized by FTIR together with CA samples at room temperature. The results of the functional group test with FTIR showed a change in the peak of the functional group, which led to the formation of a cellulose acetate functional group. Then cellulose acetate was dissolved in a mixture of acetone and DMA (4:1) which had previously been dissolved in zinc acetate, and the solution was left at room temperature until the bubbles disappeared. Next, the mixed cellulose acetate solution was put into a 10 ml syringe equipped with a 23 G needle (0.6 mm diameter) and then turned on by an electrospinning device with a voltage of 20 kV, a distance of 12 cm, and a flow speed of 0.3. ml/hour. Electrospinning was carried out for 2 h.

Furthermore, the obtained membrane was characterized by several tests, such as the contact angle test using the sessile drop method, fiber diameter measurement using FTIR, TGA, SEM, microscope Keyence test, and tensile strength test using a UTM 2 kN with wide sample dimensions. Two centimeters long and 120 mm long, measuring 80 mm long, with a test speed of 5 mm/min.

RESULTS AND DISCUSSION

Fourier-transform infrared spectroscopy (FTIR)

FTIR can provide information for predicting and identifying the functional groups present in a compound. FTIR is the easiest and fastest method for identifying chemical compounds on the membrane surfaces. An FTIR Thermo Nicolet IS50 spectrometer was used (Serial No: AUP1300076). FTIR testing was performed on the cellulose acetate samples to determine whether the cellulose acetate manufacturing process was successful by examining the functional groups in several acetate bands. Figure 3 shows the FTIR spectra of ramie cellulose converted to cellulose acetate. Figure 3 shows the acetyl groups in the bands at 1727, 1367 and 1245 cm^{-1}. This indicates that pure cellulose was converted into cellulose acetate.

Furthermore, several samples were processed by treating the difference in process temperature, as observed using FTIR. Observations showed that the esterification reaction in the synthesis process proceeded well at 25°C for 3 h. From the identification results of the C=O group in waves 1725 to 1727 cm^{-1}, the -CH_3 group in waves 1367 to 1379 cm^{-1} and the CO strain in waves 1237 to 1247 cm^{-1}; this shows a fairly high absorption (intensity), indicating the presence of acetyl groups in which the typical hydroxyl groups (-OH) of cellulose have been substituted by acetyl groups. Similar results were observed for the other two samples (temperature 40 and 80^{o}C), although there was a shift in the intensity of each peak curve.

Acetyl cellulose can be demonstrated by the presence of three vibrations of acetyl groups, namely C=O (1724 cm^{-1}) (Harahap, 2012), -CH_3 (1369 cm^{-1}) (Fei et al., 2017) and C-O (1245 cm^{-1}) (Zeng et al., 2003; Oh et al., 2015) (Figure 4b). In general, an increase in temperature causes the acetyl group to experience a decrease in the transmittance. However, for the -CH_3 and C-O groups, an increase in temperature from 40 to 80°C resulted in an increase in transmittance (Harahap, 2012; Fei et al., 2017). Table 1 shows the results of the FTIR analysis and interpretation of the membrane samples.

To confirm the above results, the FTIR spectra of the three samples were interpreted, as outlined in Table 1. The acetyl group can be interpreted as the C=O stretching band at 1725 to 1727 cm^{-1}, CH bending from CH_3 at 1267 to 1379 cm^{-1} band, and CO stretching in the band at 1237 to 1247 cm^{-1}.

Based on the results of the analysis, there was significant

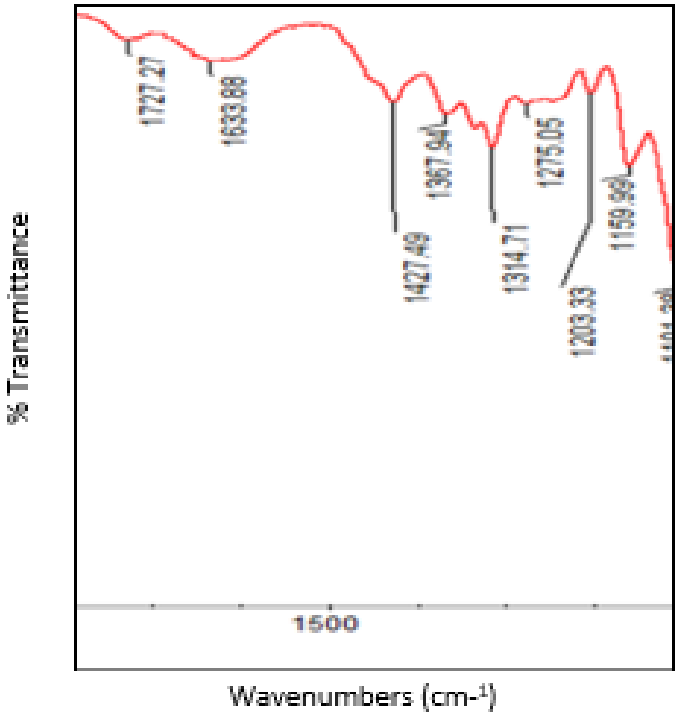

Figure 3. FTIR of Ramie based cellulose acetate (band 1200 to 1780 cm^{-1}).

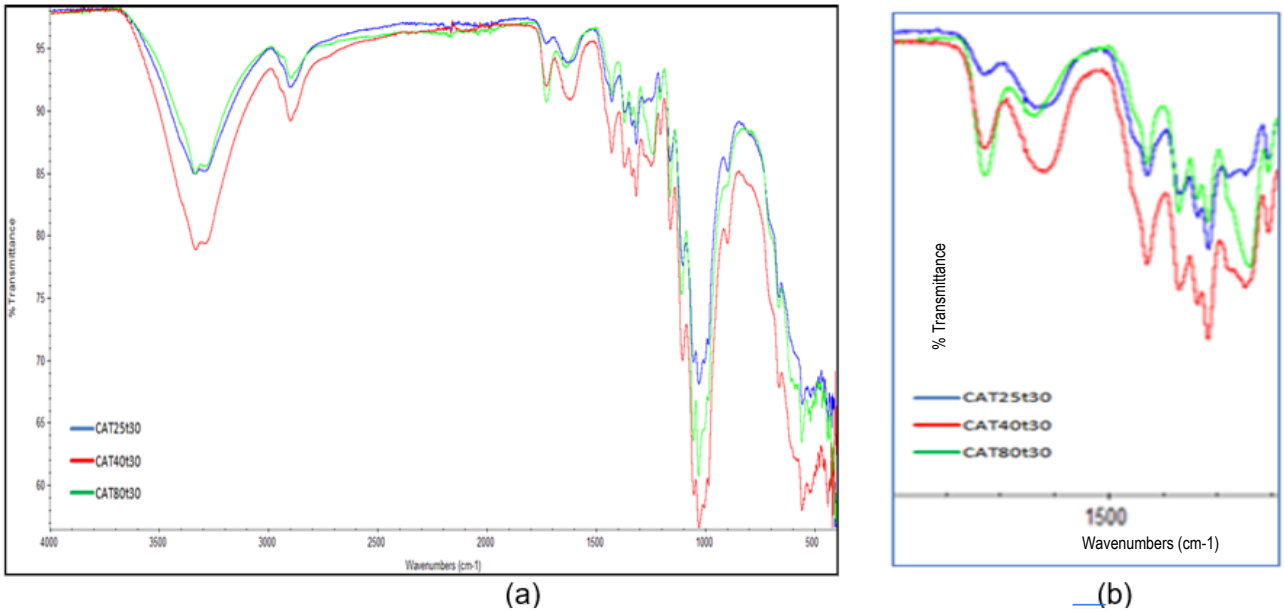

Figure 4. FTIR of cellulose acetate obtained from variation of process temperature (a) at a wavelength of 400-4000 cm^{-1} and (b) at a wavelength of 1200-1750 cm^{-1}.

a difference between the FTIR CA spectrum and the experimental results at 40 and 80°C. The absorption intensity of the hydroxyl group (–OH) decreased, whereas that of the acetyl group increased. Absorption occurred at 1730 cm^{-1}, which is characteristic of the carbonyl group (-C=O) of the ester. This indicates that qualitatively, cellulose undergoes an esterification reaction to produce CA products.

Table 1. FTIR test and interpretation of membrane samples.

Functional group	Sample CAT25t30 (cm^{-1})	Sample CAT40t30 (cm^{-1})	Sample CAT80t30 (cm^{-1})	Reference
OH stretching	3333	3331	3335	Oh et al., 2015
CH stretching	2897	2898	2896	Fei et al., 2017
C=O stretching acetyl group	1727	1727	1725	Harahap, 2012
H-O-H bending water absorbed	1633	1633	1635	Fei et al., 2017; Cheng et al., 2016
CH_2 deformation	1427	1428	1428	Yunita et al., 2018; Jo, 2016
CH bending of CH_3 on the acetyl group	1367	1369	1379	Fei et al., 2017
CO stretching on the acetyl group	1247	1247	1237	Fei et al., 2017; Oh et al., 2015
COC anti-symmetric deformation	1160	1160	1160	Celino et al., 2014
COC cellulose backbone	1052	1051	1053	Fei et al., 2017
β-link in cellulose	-	-	897	Celino et al., 2014

Thermogravimetry analysis (TGA) test

Thermogravimetric analysis uses heat-to-force reactions and physical changes in the materials. TGA provides quantitative measurements of mass changes in materials associated with thermal transitions and degradation. TGA records the changes in the mass of the dehydration, decomposition and oxidation of the sample with time and temperature. Characteristic thermogravimetric curves were obtained for certain materials and chemical compounds owing to the unique sequence of physicochemical reactions that occur over a given temperature range and heating rate. TGA Setaram Labsys Evo instrument was used in this study.

Ng, Kasi, Saidi, and Subramaniam described this in the Encyclopedia of Polymer Science and Technology (Wullandari, 2020). TGA can be used to investigate thermal stability (strength of materials at a certain temperature), oxidative stability (rate of oxygen absorption in materials), and compositional properties (e.g., fillers, polymer resins and solvents). In addition, the increase or loss of sample weight was associated with various factors. Generally, an increase in the sample weight is associated with adsorption or oxidation, whereas a decrease in sample weight is associated with decomposition, desorption, dehydration, desolvation or volatilization.

The TGA test was performed only for the nanomembrane samples obtained from a mixture of cellulose acetate (CA) and Zn acetate by electrospinning. This was performed to determine the effect of Zn on the pyrolysis of the material.

Figure 5 shows the TGA curve of the nanomembrane with ramie CA mixed with 5, 10 and 15% Zn acetate. A TGA graph of the electrospun nanomembrane mixture of cellulose acetate (CA) and Zn acetate is shown in Figure 5. Zn5 samples (nanomembranes with 5% Zn content) started to degrade at 250°C, while for the Zn10 and Zn15 samples, degradation started to occur at 280°C. An increase in the Zn content of the nanomembrane affected the temperature at which the material began to degrade.

This is in accordance with previous studies showing that pure cellulose will be degraded at a temperature of approximately 250°C and after 350°C, the remaining residue decomposes at a slow rate of degradation (not a significant decrease in the curve) (Ramahdita et al., 2017). In Figure 5, It can also be seen that the resulting Zn5 sample experienced a mass decrease of +51% at 350°C and ±64% at 550°C. Meanwhile, the resulting Zn10 samples decreased by ±50% at 350°C and ±52% at 550°C. In contrast to the two previous samples (Zn5 and Zn10), the Zn15 sample experienced mass decreases of±11% at 350°C and ±18% at 550°C, or it indicating that the residue of the Zn15 sample was still ±82% at 550°C. This indicates that Zn (15%) is highly influential in reducing the level of material degradation. It can be said that the Zn15 sample was more heat- or fire-resistant. Nanomembranes with the ability to retain heat may be used as mask materials for firefighters.

Scanning electron microscopy (SEM)

A JEOL JSM 6360 LA scanning electron microscope (SEM) was used. SEM has a higher resolution than optical microscopy. This is due to the de Broglie wavelength, which has fewer

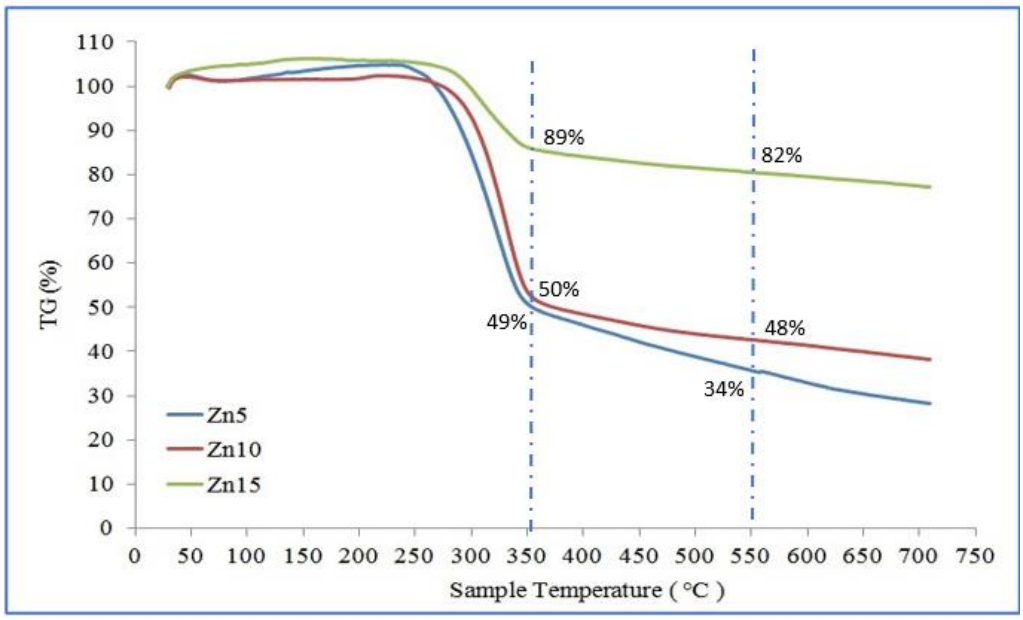

Figure 5. TGA results of nanomembrane samples with Zn acetate

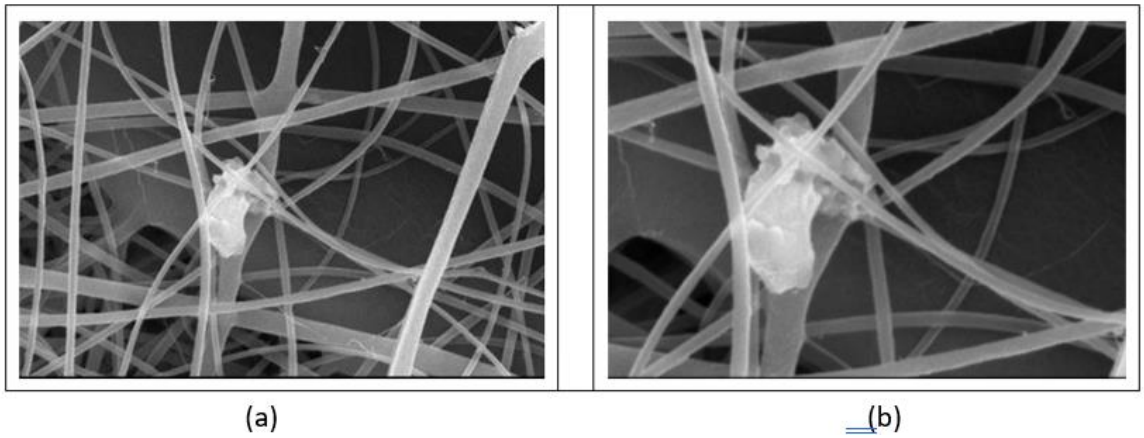

Figure 6. SEM testing of Ramie fiber nanomembrane (a) 5000X magnification, (b) 9000X magnification.

electrons than optical waves. The smaller the wavelength, the higher the resolution of the microscope. SEM has a large depth of field, which can focus on a larger number of samples at one time and produce good images of three-dimensional samples (Anonim, 2012). There was appearance of the membrane in SEM observations at 5000 and 9000x magnification.

SEM testing was performed on the membranes resulting from the electrospinning process using ramie cellulose acetate fibers to measure the number of fibers formed. In Figure 6, it can be seen that at 5000X magnification, fibers of various sizes are quite clear even though there is little impurity (a), and at 9000X magnification, fiber variations are quite clear and the impurities are probably in the form of beads (b).

Increasing the tension can indeed increase the productivity of the resulting fiber; however, this has several problems, including the difficulty of forming Taylor cones owing to the large tensile force from the electric force, which cannot be balanced by the surface tension of the solution. As a result, electrospinning and electrospraying, which can be seen from the presence of "stains" on the electrospinning results. To obtain nanomembranes that are even and clean from beads, it is necessary to optimize the process conditions by synchronizing voltage, solution supply, and solution

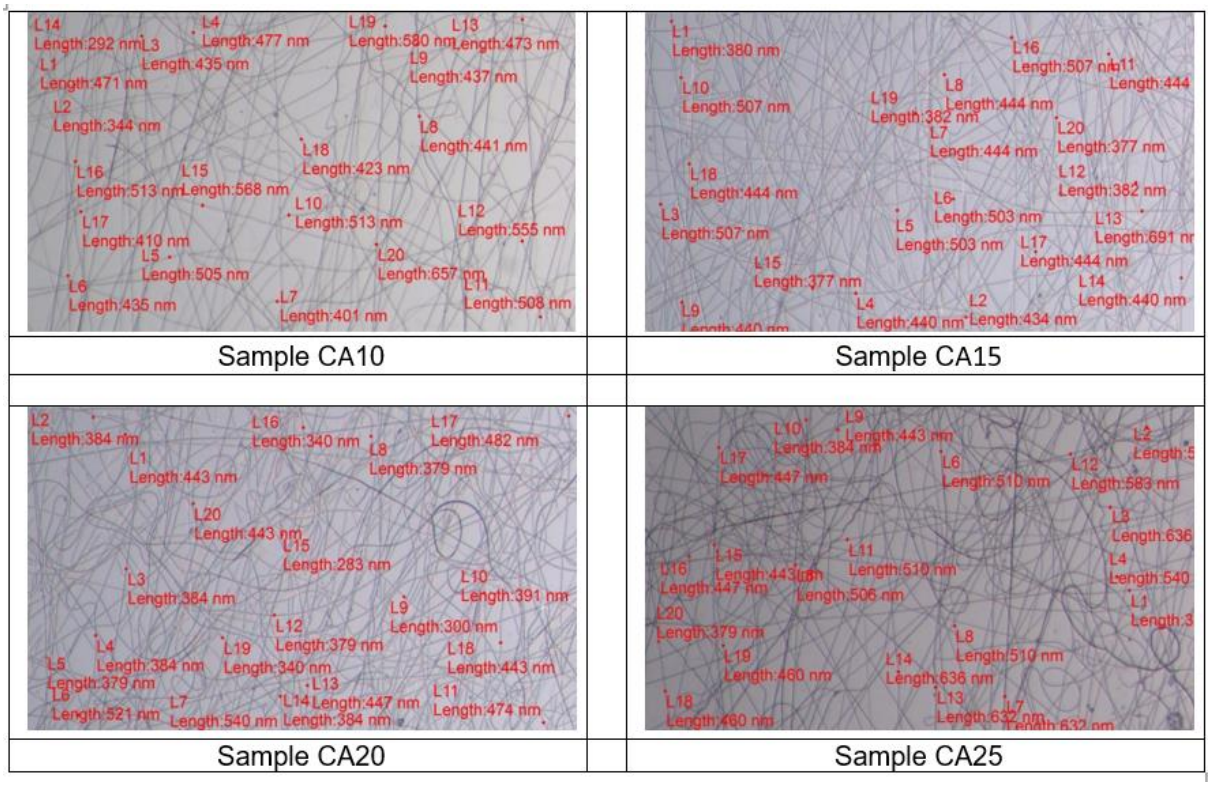

Figure 7. Polarization microscope testing of nanomembranes.

viscosity. In this study, fiber size measurements were carried out using a "Keyence" polarizing microscope.

Microscope Keyence test

The polarizing microscope (MP) "Keyence" is one of the tools used to meet the needs of small-material observations with fairly high accuracy. The diameter of the fibers was measured using ImageJ software. ImageJ is a powerful software package used for image analysis. The image quality obtained using the Keyence Polarizing Microscope and 3D Laser Scanning Microscope (Keyence VK-X1000) is similar to the observations with SEM, but the cost is cheaper than using SEM. Illumination was set to the full coaxial mode, and the white balance was adjusted prior to imaging using an MP with a cross polarizer. Electrospun fiber imaging was performed at 1100x magnification (Nguyen et al., 2020).

The electrospinning process used a flow rate of 1 ml/hour with varying voltages, and the fiber diameter was observed using ImageJ software. The results of the observations with a polarizing microscope from the CA10, CA15, CA20 and CA25 samples at a flow rate of 1 ml/h are shown in Figure 7. The results of the fiber diameter measurements using ImageJ software are shown in Table 2.

Figure 7 shows the results of observations using a polarizing microscope for samples CA10, CA15, CA20 and CA25. Observations show that electrospinning produces fibers with diameters ranging from 100 to 300 nm. Table 2 shows that with a population of 20 measurements per sample, the average fiber diameter obtained in samples CA10, CA15 is 308 nm, CA20 is 305 nm and CA25 was 286, 308, 305 and 308 nm, respectively, with a standard deviation of 41 to 49.

Furthermore, the fiber diameter data in Table 2 were grouped according to sizes of 0 - 100, 100 - 200, 200 - 300, and 300 - 400 µm; the recapitulation results are presented in Table 3. The electrospinning process in this study produced fibers with sizes mostly between 200 and 300 nm in all four samples, and in the CA10 sample, it reached 70%. In the CA15, CA20 and CA25 samples, the fiber diameters in the 200 to 300 and 300 to 400 nm groups were equally divided. Interestingly, the CA10 and CA15 samples also exhibited diameters of < 200 nm, although not significantly so.

This research was also attempted using a flow rate of 2 ml/hour, and the voltage was the same as that used with a flow rate of 1 ml/hour previously. The results were not better, but decreased when the percentage of fiber diameter produced was larger in diameters between 300 and 400 nm and there was even a small percentage with a size of 500 to 600 nm. Thus, it can be concluded that in

Table 2. Observation results of fiber size using a polarizing microscope test.

No.	Fiber diameter (nm)			
	Ca10	**CA15**	**CA20**	**CA25**
1.	216	379	284	284
2.	320	332	288	379
3.	284	332	331	284
4.	276	237	284	331
5.	288	332	331	284
6.	300	284	382	331
7.	284	381	335	284
8.	384	381	241	284
9.	331	333	284	331
10.	189	237	335	284
11.	288	288	223	237
12.	281	237	284	331
13.	281	237	325	331
14.	281	284	335	331
15.	256	379	335	379
16.	356	285	279	284
17.	213	248	357	284
18.	356	238	254	237
19.	250	285	284	284
20.	284	135	335	384
Average	**286**	**308**	**305**	**308**
Std dev.	49	42	41	42
Error	11	10	9	10

Table 3. Recapitulation of fiber diameters.

Sample (kV)	Percentage of fiber diameter (%)			
	0 - 100 nm	**100 - 200 nm**	**200 - 300 nm**	**300 - 400 nm**
10	0	5	70	25
15	0	5	55	40
20	0	0	50	50
25	0	0	55	45

this study, a flow rate of 1 ml/hour with a voltage of 10 kV was the optimal condition for electrospinning to produce nanosized fibers. Nanomembranes produced from 100 to 400 nm nanofibers can filter micron-sized bacteria and also nano-sized viruses.

Sessile drop test

Furthermore, nanomembrane samples were tested with water droplets using the sessile drop method (Dataphysics, 2017). The sessile drop test is intended to determine the ability of a membrane to retain water or droplets when water drops onto its surface. This test is structured as follows; Droplets of 5.0 L of the test liquid are placed on the coated cloth and a profile image of the drop is obtained using an optical system, in this case a camera equipped with a macro lens. This process was repeated thrice. The contact angle was measured using ImageJ software version 1.52 using the LAB-ADSA Drop Analysis plugin.

Continuous measurement of the contact angle and contact angle length without change is an indicator of whether the surface of an object is waterproof or impermeable. Note that, in Figure 8, the surface of the object (membrane) with a contact angle > 1000° lasted for more than 15 min. From the results of the sessile drop test, where the average contact angle was above 1000

Figure 8. Contact angle of nanomembrane after sessile drop test

Table 4. Comparison of tensile strength of nanomembrane before and after mixed Zn.

Sample	Max load (N)	Speed (mm/min)	Area (mm^2)	Tensile strength (N/mm^2)	Ultimate elongation (%)
Nanomembrane-1	0.207	5	0.420	0.492	1,015
Nanomembrane-2	0.251	5	0.498	0.504	1,053
Average	**0.229**		**0.459**	**0.498**	**1,034**
Nanomembrane + Zn5-1	0.467	5	0.419	1.116	5,126
Nanomembrane + Zn5-2	0.431	5	0.559	0.770	2,199
Average	**0.449**		**0.489**	**0.943**	**3,663**

from three measurements of 141.30°, as shown in Figure 8, it can be concluded that the nanomembrane has an indication of water resistance or water repellency.

Nanomembranes with waterproof properties can be applied to mask filters for the medical field. A mask with waterproof properties will prevent fluid or blood from splashing onto the user during surgery or other medical activities.

Tensile strength test (ASTM 882-91, 1996)

A tensile strength test of the membrane was performed to obtain data on the strength and elongation of the membrane, which will be used as a material consideration in determining the choice of membrane application. Tensile strength and elongation were determined using a universal testing machine (UTM Gotech Al-7000-S). Film specimens (8 × 0.5 cm) were cut from each sample and placed between the handles of the machine. The tensile strength was determined based on the maximum load when the film broke and the elongation percentage was determined based on the elongation of the film when the film broke. The parameters used to determine the mechanical properties of the membrane are stress, strain, and Young's modulus. To obtain the results for these parameters, the material or membrane is stretched, the reaction of the material to the tensile force (force/F) is obtained, and the change in the length of the material after being pulled (Δl) (Callister et al., 2007).

Ramie CA nanofiber membranes have relatively low mechanical strength, possibly because of their amorphous shape, as the fibers are not bonded to each other. To overcome this problem, the nanofiber membrane is heated below its melting point to dry so that the nanofiber membranes are more bonded to each other and maintain their morphology. However, temperatures above the melting point (210°C) can easily destroy the material (Ma et al., 2005).

The tensile strength was measured using a UTM of 2 kN with sample dimensions of 2 cm width, 120 mm length and 80 mm length at a test speed of 5 mm/min. The tensile strength of the nanomembranes was compared between CA nanomembranes and nanomembranes with the addition of Zn (5%). The results of the strength measurements are presented in Table 4. From the tensile strength measurements of the Zn5 sample, it was found that the tensile strength of the sample Zn5 increased almost 2 times as much as the tensile strength of the CA Ramie nanomembrane sample without Zn (CAT40t30). Similarly, the elongation of the Zn5 sample increased to 3.663% or 3.5 of that of the CA nanomembrane (1.034%). Another effect is that the addition of Zn increases the area by 0.040 mm^2 or 8.71%, which can also affect the maximum load of the nanomembrane samples with 5% added Zn.

As previously discussed, the use of membranes is very broad, namely in the fields of health, food, water and wastewater treatment, and the chemical industry, as well as other fields of biotechnology. The nanomembrane made from cellulose acetate and Zn in this research has

high strength and elasticity, so this nanomembrane is very qualified for use in areas that experience a lot of mechanical stress, such as tension and compression.

Conclusion

This method was chosen because it is easier and can produce nanosized fibers compared with other methods. In addition, this method reduces water use, saves raw materials, and wastes relatively little material, making it environmentally friendly.

This research has been able to produce nanomembranes with fiber sizes between 200 and 400 nm, so they are quite good as filters for filtering small materials. The advantage of nanofiber membranes made from hemp fiber is that the raw material comes from natural fibers so it is sustainable and biodegradable; this means that these materials can be renewed and decomposed in nature.

The characterization results of cellulose acetate and Zn based nanomembranes have high strength and elasticity, are high temperature resistant and also water resistant, so that the resulting nanomembranes can be used for the medical field (filter mask and/or wound dressing), as well as masks for firefighters.

Although several interesting possibilities have been discovered, some of them remain unexplored. Future research aimed at the application of membrane technology, the utilization of natural fibers, and the study of additive components in fiber structures for various applications needs to be considered.

CONFLICT OF INTERESTS

The authors have not declared any conflict of interests.

ACKNOWLEDGMENT

The author would like to thank the Ministry of Research and Technology – Republic of Indonesia/National Research and Innovation Agency, for the approval of the Implementation of the Ramie Fibre-Based Green Textile PRN Program in 2020 to obtain funding from the Education Fund Management Institute (LPDP), and the Director of the Research Centre for Advanced Material (BRIN), which has allowed them to carry out activities at the PRMM Laboratory, as well as the Ramie Consortium and friends who collaborated to make this program a success.

REFERENCES

Anonim (2012). SEM (Mikroskop Elektron Scanning). http://mandeleyevrapuan.blogspot.com.

Astuti BC (2008). Pengembangan edible film kitosan dengan penambahan asam lemak dan esensial oil: upaya perbaikan sifat barrier dan aktivitas antimikroba. Skripsi. Bogor: Fakultas Teknologi Pertanian Institut Pertanian Bogor.

Callister WD, Rethwisch DG, Blicblau A, Bruggeman K, Cortie M, Long J, Mitchell R (2007). Materials science and engineering: an introduction, New York: John Wiley and Sons 7:665-715.

Celino A, Gonçalves O, Jacquemin F, Fréour S (2014). Qualitative and quantitative assesment of water sorption in natural fiber using ATR-FTIR spectroscopy. Carbohydrate Polymers 101:163-170.

Chen G, Ushida T, Tateishi T (2002). Scaffold design for tissue engineering. Macromolecular Bioscience 2(2):67-77.

Cheng S, Huang A, Wang S, Zhang Q (2016). Effect of different heat treatment temperatures on the chemical composition and structure of Chinese fir wood. BioResources 11(2):4006-4016.

Coutinho Cesar de M (2009). State of Art of the Apllications of Membrane Technology to Vegetable Oils. Brazil: State University of Campinas Department of Food Technology Laboratory of Fats and Oils (LOG).

Dataphysics (2017). Sessile drop method - optical determination of the contact angle. http://www.dataphysics.de/2/start/understanding-interfaces/drop-shape-analysis/sessile-dropmethod/.

Deitzel JM, Kleinmeyer J, Harris D, Beck Tan NC (2001). The effect of processing variables on the morphology of electrospun nanofibers and textiles. Polymer 42(1):261-272.

Dersch R, Steinhart M, Boudriot U, Greiner A, Wendorff JH (2005). Nanoprocessing of polymers: Applications in medicine, sensors, catalysis, photonics. Polymers for Advanced Technologies 16(2-3):276-282.

Drioli E, Lidietta G (2010). Comprehensive Membrane Science and Engineering. United Kingdom: Vol. 1 Elsevier B.V.

Fei P, Liao L, Cheng B, Song J (2017). Quantitative analysis of cellulose acetate with a high degree of substitution by FTIR and its application. Analytical Methods 9(43):6194-6201.

Habibie S, Suhendra N, Roseno S, Setyawan BA, Anggaravidya M, Rohman S, Tasomara R, Muntarto A (2021a) Serat alam sebagai bahan komposit ramah lingkungan, suatu kajian pustaka. Jurnal Inovasi dan Teknologi Material 2(2):1-13.

Habibie S, Suhendra N, Setiawan BA, Hamzah M, Aisah N, Fitriani DA., Tasomara R, Anggaravidya M (2021b). Prospect of Ramie Fiber Development in Indonesia and Manufacturing of Ramie Fiber Textile-based Composites for Industrial Needs, an Overview. International Journal of Composite Materials 11(3):43-53.

Handayani SS, Tarnanda R, Rahayu BA (2018). Amrullah,"The process of delignification of lignin in tobacco stem waste as preparation for ethanol production. Jurnal Oijar MIPA 13(2):140-146.

Harahap M (2012). Pembuatan Selulosa Asetat dari A-Selulosa yang Diisolasi dari Tandan Kosong Sawit (Doctoral dissertation, Universitas Sumatera Utara).

Jo JS, Jung JY, Byun JH, Lim BK, Yang JK (2016). Preparation of cellulose acetate produced from lignocellulosic biomass. Journal of the Korean Wood Science and Technology 44(2):241-252.

Karakoc V, Yavuz H, Denizli A (2004). Affinity adsorption of recombinant human interferon-alpha on a porous dye-affinity adsorbent. Colloids Surf A 240:93.

Kumano A, Fujiwara N (2008). Cellulose Triacetate Membranes for Reverse Osmosis. In Advanced Membrane Technology and Applications; Li NN, Fane AG, Ho WSW, Matsuura T (2008). Eds.; John Wiley & Sons: Hoboken, NJ, USA pp. 21-46.

Lankaster M (2002). Green Chemistry. RSC Paperbacks. Cambridge.

Li D, Wang Y, Xia Y (2003). Electrospinning of polymeric and ceramic nanofibers as uniaxially aligned arrays. Nano letters 3(8):1167-1171.

Liu ZT, Fan X, Wu J, Zhang L, Song L, Gao Z, Tang S (2007). A green route to prepare cellulose acetate particle from ramie fiber. Reactive and Functional Polymers 67(2):104-112.

Lu T, Cui J, Qu Q, Wang Y, Zhang J, Xiong R, Ma W, Huang C (2021). Multistructured Electrospun Nanofibers for Air Filtration: A Review. ACS Applied Materials and Interfaces 13(20):23293-23313.

Ma X, Yu J, Kennedy JF (2005). Studies on the properties of natural fibers-reinforced thermoplastic starch composites. Carbohydrate Polymers 62(1):19-24.

Ma Z, Kotaki M, Ramakrishna S (2005). Electrospun cellulose nanofiber as affinity membrane. Journal of Membrane Science, Elsevier.

Matthews JA, Wnek GE, Simpson DG, Bowlin GL (2002).

Electrospinning of collagen nanofibers. Biomacromolecules 3(2):232-8. Doi: 10.1021/bm015533u.

Muryanto M, Sudiyani Y, Abimanyu H (2016). Optimization of the NaOH pre-treatment process of oil palm empty fruit bunches to become bioethanol. Jurnal Kimia Terapan Indonesia 18(01):27-35.

Nguyen J, Stwodah RM, Vasey CL, Rabatin BE, Atherton B, D'Angelo PA, Swana KW, Tang C (2020). Thermochromic Fibers via Electrospinning. Polymers 12(842):1-15. doi:10.3390/polym12040842.

Nunes PS, Peinemann KV (2001). Membrane Technology in the chemical industry. New York: Jon Willey & Sons.

Oh SY, Yoo DI, Shin Y, Seo G (2005). FTIR analysis of cellulose treated with sodium hydroxide and carbon dioxide. Carbohydrate Research 340(3):417-428.

Ramahdita G, Ilmiati S, Suryanegara L, Khalid A, Chalid M (2017). Preparation and characterization for sorgum-based micro-fibrillated celluloses. Macromol Symp, 371:69-74.

Setyaningrum A, Sumarni NK, Hardi J (2017). Sifat Fisiko-Kimia Edible Film Agar–Agar Rumput Laut (*Gracilaria* sp.) Tersubtitusi Glyserol. Natural Science: Journal of Science and Technology 6(2):136-143.

Stankus JJ, Guan J, Wagner WR (2004). Fabrication of biodegradable elastomeric scaffolds with submicron morphologies. Journal of Biomedical Materials Research Part A 70(4):603-614. DOI: 10.1002/jbm.a.30122.

Suen SY, Liu YC, Chang CS (2003). Exploiting immobilized metal affinity membranes for the isolation or purification of therapeutically relevant specie. Journal of Chromatography B 797(1-2):305-319.

Sunthornvarabhas J, Chatakanonda P, Piyachomkwan K, Sriroth K (2011). Electrospun polylactic acid and cassava starch fiber by conjugated solvent technique. Materials Letters 65(6):985-987.

Taylor GI (1969). Electrically driven jets. Proceedings of the Royal Society of London. A. Mathematical and Physical Sciences 313(1515):453-475.

Um IC, Fang D, Hsiao BS, Okamoto A, Chu B (2004). Electro-spinning and electro-blowing of hyaluronic acid. Biomacromolecules 5(4):1428-36. doi: 10.1021/bm034539b.

Wullandari P (2020). Peneliti LRMPHP (http://www.mekanisasikp.web.id/2020/03/mengenal-tga-thermogravimetric-analysis.html).

Xia B, Zhang G, Zhang F (2003). Bilirubin removal by Cibacron Blue F3GA attached nylon-based hydrophilic affinity membrane. Journal of Membrane Science 226:9-20. https://doi.org/10.1016/j.memsci.2003.08.007

Yuan J, Dunn D, Clipse NM, Newton Jr RJ (2009). Characterization of Cellulose Acetate Films: Formulation Effects on the Thermomechanical Properties and Permeability of Free Films abd Coating Films. Pharmaceutical Technology 33(3):88-100.

Yunita RF, Nasution DY, Marpongahtun M (2018). Manufacturing and characterization of cellulose acetate from oil palm logs (*Elaeis Guinensis* Jack) with Chloroform as solvent and triacetin as plasticizer. International Journal of Science Technology and Engineering 4(8):86-91.

Zakrzewska A, Haghighat BMA, Nakielski P, Petronella F, De Sio L, Pierini F (2022). Nanotechnology transition roadmap toward multifunctional stimuli-responsive face masks. ACS Applied Materials and Interfaces 14(41):46123-46144.

Zhang X, Reagan MR, Kaplan DL (2009). Electrospun silk biomaterial scaffolds for regenerative medicine. Advanced Drug Delivery Reviews 61(12):988-1006.